CHAPTER IV

TUNNEL INDUCED GROUND MOVEMENTS

The construction of tunnels or surface excavations in soft ground will lead to ground movements. However, the magnitude of soil movements depends mainly on the size of the opening, the distance to the excavation and the properties of the soil itself which is located around the construction site. This chapter describes the mode of soil displacements given by two model tests for the tunnel in clay and in sand as well as the different sources of ground movements generated by shield tunneling. An overview of different methods developed and used to estimate the ground surface and subsurface movements are also given in this chapter.

4.1 Causes of Soil Displacements around Tunnels in Soft Soil

4.1.1 Displacement Victors in Soft Soils

The word soft soil may refer to one or both of cohesive and granular soils. However, the previous research studies typically classified soft soil into only one of them even there is no such one layer of soil in reality. The victors of ground movements in response to the tunnel excavation in the two types of soils may be distinguished by two model tests (Figure 4.1), which were conducted by Mair (1979) and Potts (1976) and cited by O'Reilly and New (1982). The movements appearing in cohesive soil seem directed towards a sink located at a point somewhere below axis level of the tunnel. However, the width of the settlement is wider than that of the cohesionless soil where the movements seem to be deeper and narrower.

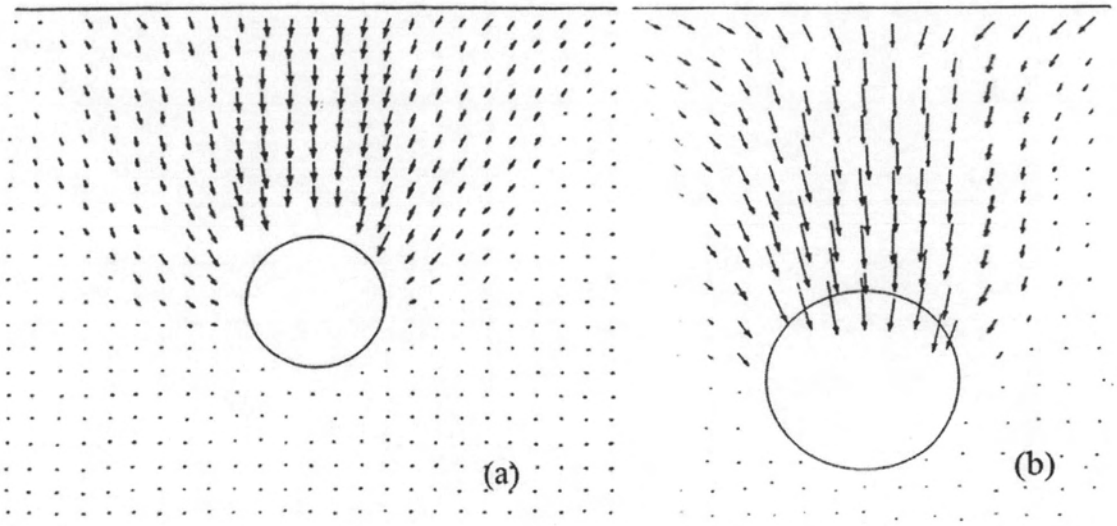

Figure 4.1 Victors of soil displacements around model tunnel (a) in clay (Mair, 1979) and (b) in sand (Potts, 1976) (cited by O'Reilly and New, 1982)

4.1.2 Causes of Soil Displacements

The ground movements due to shield tunneling in soft soil are closely related to the ground loss, which is affected by the combination of various factors (Figure 4.2). According to Suwansawat (2002) and the real excavation process, the fundamental ground loss could be described as:

- Ground loss at the shield face (Figure 4.2a): Face loss into the tunnel develops when an open-face shield is used, or if the shield is operated at low support pressure so that the soil is allowed to move towards the face from a zone of influence ahead. In this condition, the volume balance is negative, or more volume of soil is removed than is occupied by the shield advance.
- Ground loss due to over-cutting (Figure 4.2b): In order to advance the shield it is necessary to have an over-excavation outside the tunnel perimeter at the face of the machine. This is accomplished by the presence of copy cutters, which could be extended up to 185 mm outside the perimeter of the cutting wheel according to the dimension of the shield and the machine construction techniques.
- Ground loss due to pitching (Figure 4.2c): Plowing or yawing of the machine caused by pitching can cut an ellipse of larger cross-sectional area than the area of the shield. At the same pitching angle, a shield with longer

length theoretically introduces a larger gap over its shield than a shield of shorter length.

- Ground loss due to ground disturbance (Figure 4.2d): After the cutting wheel has passed, a disturbed or remolded zone around the shield surface due to shoving of the large diameter shield can cause ground movement over the shield body.
- Ground loss due to tail void closing (Figure 4.2e): The tail void after shield passing causes an additional component of ground deformation due to closure of the soil into the gap. The void is created by the difference between the excavated periphery and the permanent outer liner surface. One usually tries to eliminate the gap by expanding the lining or by grouting around the lining as it emerges from the tail of the shield, before the soil displaces into the gap.

The magnitude of ground movements that occur from these different phases is mainly influenced by ground conditions, the construction method, and shield operation control. Operation control includes the pressure control at the face, the steering of the shield, penetration rate, and quality of workmanship. Hence, allowing movements into the face of the tunnel, introducing tail void enlargement, greater soil disturbance by poor steering practices, and slow installation of the liner due to the poor operation all lead to an increase in ground movements.

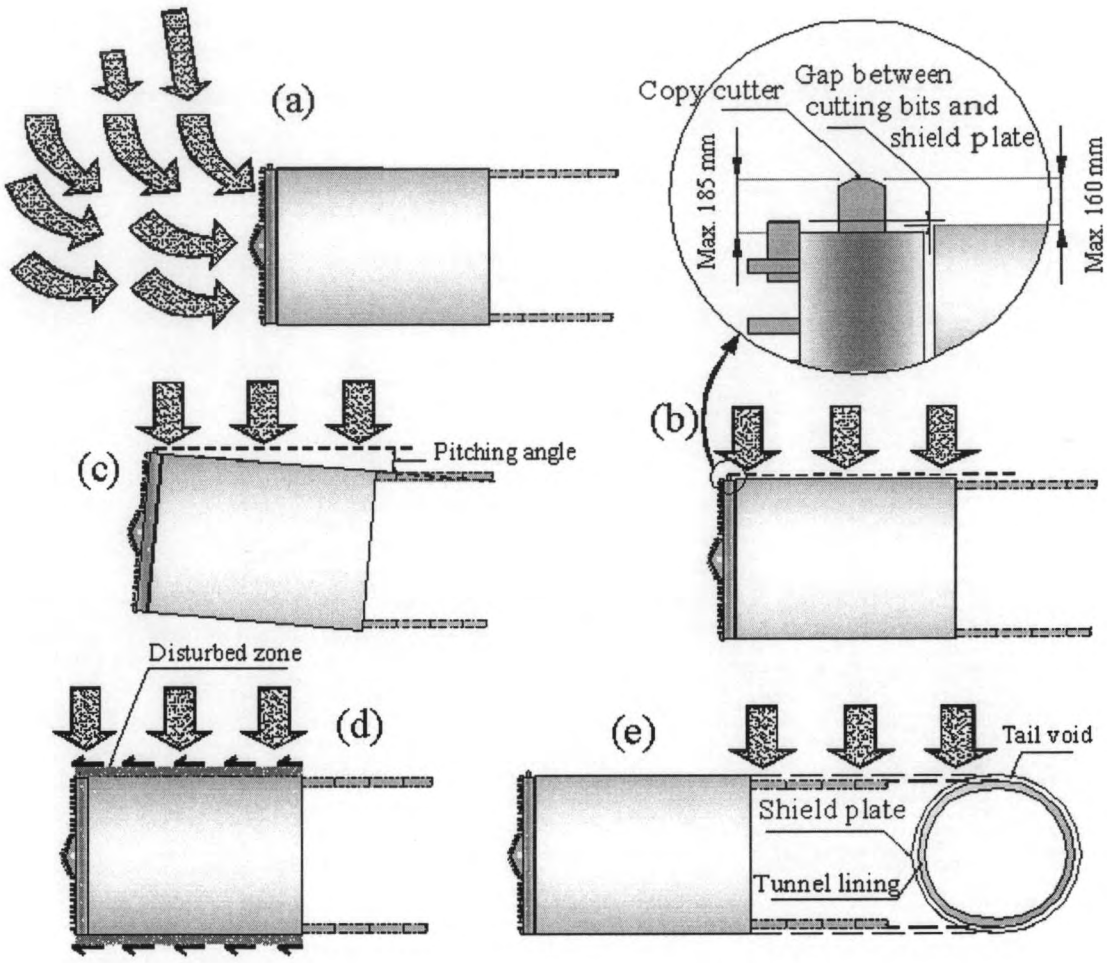

Figure 4.2 Causes of ground loss during shield tunneling

Similarly, in the Japanese Standard for Shield Tunneling (JSST), which was published by the Japan Society of Civil Engineers (JSCE, 1996), the third edition, the causes of soil displacements could be separated in five main points. Though some causes are exactly the same as what have been described previously, other causes are clearly and complimentarily mentioned to be considered for identifying the sources of ground loss or ground movements. These causes are described as follows:

1.) Unbalanced ground and groundwater pressure at face: if the shield advancement rate and muck discharge rate are not synchronized in an EPB shield or slurry shield, the pressure inside the chamber becomes different from the ground and groundwater pressure, at the face become unbalanced, which causes ground movements. If the pressure in the chamber is smaller than the ground pressure, surface settlement occurs. In cases of contrary,

ground heave occurs. These phenomena are due to pressure release at the face and elasto-plastic deformation by an additional pressure.

2.) Ground disturbance during advancement: ground disturbance due to shield advancement and friction between the skin plate of the shield machine and ground may cause ground heave or settlement. Especially, extra excavation for alignment control or driving through a curved section causes ground loosing.

3.) Occurrence of tail void and insufficiency of backfill grouting: due to an occurrence of tail void, the ground which is supported by a skin plate, it causes deformation and ground settlement occurs. This is an elastic deformation caused by stress relief. The magnitude of ground settlement depends on the backfill grouting material, timing, grouting locations, pressure and grouted volume. Excessive pressure of backfill grouting in clayey ground may cause ground heave.

4.) Deformation and displacement of the primary lining: if joint bolts are not fully tightened, a segmental ring tends to be deformed. This increases ground settlement, as the nominal area of the tail void increases or the primary lining deforms due to unbalanced loads, after it is pushed out from the tail.

5.) Decline of groundwater table: if water flows in from the cutting face or leaks through the primary lining, the groundwater table declines, which causes ground settlement. This settlement is caused by consolidation, as the effective stress of the ground increases.

Based on the above mentioned causes (JSCE, 1996), the consequences of ground movements could be plotted in 5 different stages of occurring: i) and ii) prior to the passage of the shield machine, iii) during the passage, iv) and v) after the shield machine has passes.

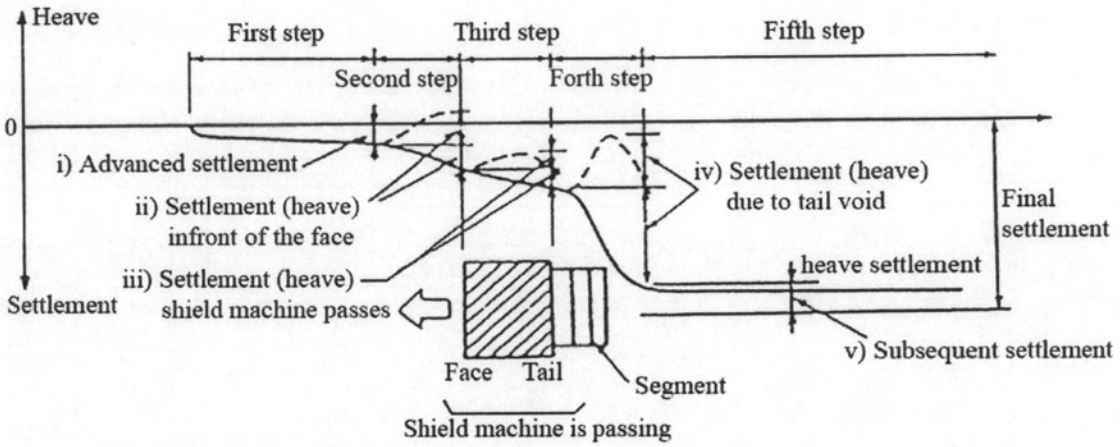

Figure 4.3 Ground movements due to shield advancement (JSCE, 1996)

The successive movements shown in Figure 4.3 could be described briefly as follows:

i) Advanced settlement: this occurs well in advance before the shield machine passes. It is caused by the decline of groundwater table in sandy ground. In extremely soft clayey ground, it may occur as ground flows in at the face.

ii) Settlement (or heave) in front of the face: this type of settlement or heave occurs just before the shield machine passes, which is caused by unbalanced pressures of ground and groundwater at the face.

iii) Settlement (or heave) shield machine passes: this is caused by friction between the shield machine and ground or disturbance of the ground due to over-excavation.

iv) Settlement (or heave) due to tail void: settlement or heave occurs immediately after the shield tail has passed. It is caused by stress relief because of tail void or by excessive backfill grouting pressure. This type of settlement is the most important settlement in shield tunneling.

v) Subsequent settlement: this settlement occurs in soft clayey ground. Loosening or disturbance of the ground is the main cause.

(JSCE, 1996)

The magnitude and distribution of ground settlement vary depending on ground conditions, the ratio of overburden depth to shield diameter, boring condition as well as percent of ground loss and tail void.

Teparaksa (2005a) simply classified the ground surface and subsurface movements into three portions (as shown in Figure 4.4) due to EPB tunneling in Bangkok subsoils for MRTA project as:

1.) portion 1: settlement about 10% caused by soil flow into the shield.
2.) portion 2: settlement about 20% caused by soil displacement during installation of segmental lining.
3.) portion 3: major settlement about 70% caused by soil tail void after TBM passing.

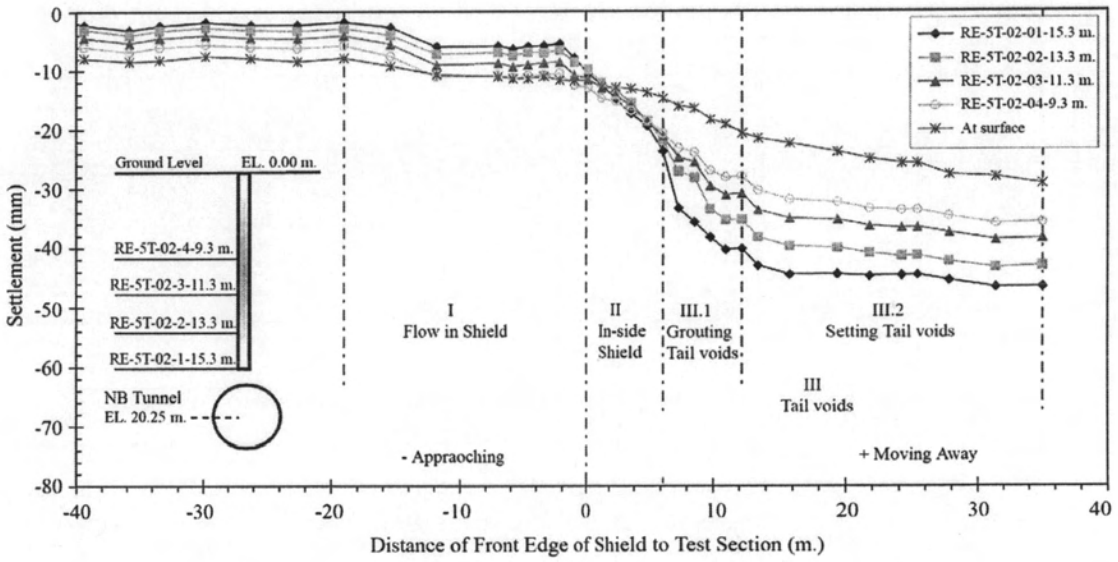

Figure 4.4: Behaviors of ground displacements caused by EPB tunneling (Teparaksa, 2005a)

Although the causes of soil displacements have been known, there is no measure to eliminate these phenomena. However, the excessive displacements could be reduced based on experiences of the shield operator and the workman shift.

4.2 Predicting Methods of Ground Displacements

The understanding of ground and structural displacement mechanisms is necessary since it helps the constructor to prepare the preventive measures in order to assure the normal function of public activities at the ground surface. Therefore, the appropriate predicting method is needed for accurately estimating the magnitude of

ground as well as structural movements before starting a tunnel construction. Until now, four kinds have been established as predicting methods, which have been used for this purpose. First, the empirical methods are proposed based on the case history of field monitored data, and normal contribution curve is used to compute the ground settlement trough. Secondly, the analytical methods (closed-form) of which the ground displacements are determined analytically. Thirdly, the Finite Element Methods (FEMs) have been extensively employed since it provides not only the ground surface movements, but also the subsurface movements. In addition, the various obstructions, i.e. buildings, structures and foundations, at ground surface and subsurface of the analysis section can be input into the model that allows designers to know in advance the tendency of those structure movements in response to the tunnel excavation. Finally, the laboratory tests, which are based on the centrifuge models to simulate the tunnel excavation and ground movements and the results obtained from the tests could be suggested for predicting the maximum surface settlements as well as the form of soil movement around the tunnel. However, the time consumed for sample preparation and the number of experiments carried out is very long. Moreover, it is difficult to simulate the real tunnel excavation and to implement the surface and subsurface structures into the model.

In general the ground surface settlement trough above and ahead of the advancing tunnel for a single tunnel in green-field site (place where there has been no previous surface or subsurface construction) is manifested as shown in Figure 4.5 (Attewell et al., 1986).

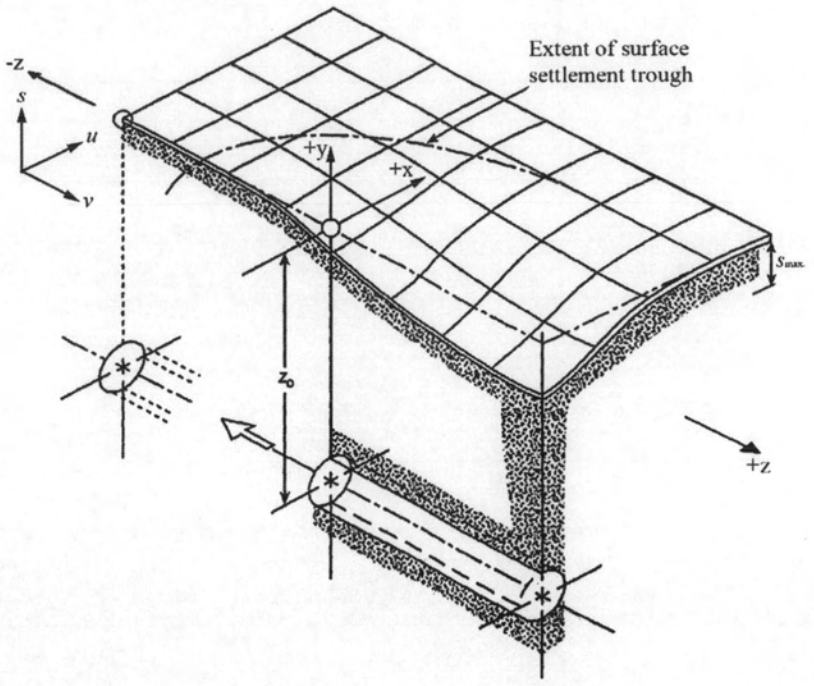

Figure 4.5 Settlement trough above an advancing tunnel (Attewell et al., 1986)

4.2.1 Empirical Methods

Several empirical methods have been developed based on the error function or normal probability curve (sometime it is called Gaussian curve) to predict the ground movements in respond to tunnel construction. However, for surface settlement, only the approach suggested by Peck (1969) and the extension developed by O'Reilly and New (1982) will be reviewed here. For subsurface settlement, the development work made by Mair et al. (1993) will be described. These approaches have been extensively used for estimating the ground surface settlements in many research studies.

Peck (1969) reported a study of ground surface settlement data, which were available from more than twenty case histories during that time, and led to a conclusion that the settlement trough induced by a single tunnel excavation could be presented by the error function or normal probability curve. Until now, this empirical approach is still widely used to predict the ground surface settlements resulting from tunnel excavation in soft ground. The vertical settlement "*s*" in the transverse direction is defined as

$$s = s_{max} \exp(\frac{-x^2}{2.i^2}) \qquad (4.1)$$

where, s_{max} is the maximum settlement measured above the tunnel axis (at x = 0), x is the transverse distance from the tunnel axis and i is the standard deviation of the normal distribution curve. The value of i gives a means of defining the settlement trough width and equals to x at the point of inflection of the curve. In practice, the total half-width of settlement trough is given by about $2.5i$. Figure 4.6 shows a typical transverse settlement trough above a single tunnel located at a depth of z_0 from ground surface and R is the radius of the tunnel.

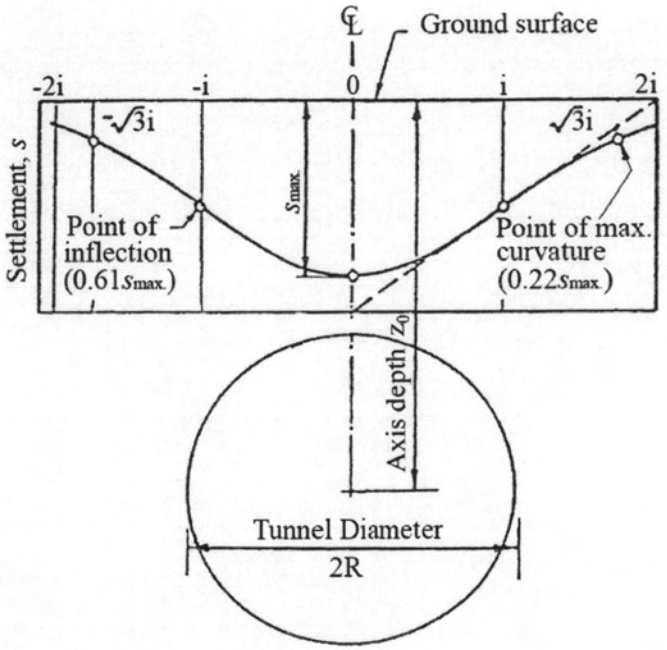

Figure 4.6 Transverse settlement trough (Peck, 1969)

The values of i had been calculated for tunnels above which reasonably reliable settlement data were available. They are illustrated in a dimensionless plot of i/R against $z_0/2R$ for different soil conditions (Figure 4.7). It can be seen that the settlement trough width parameter becomes wider for a deeper tunnel.

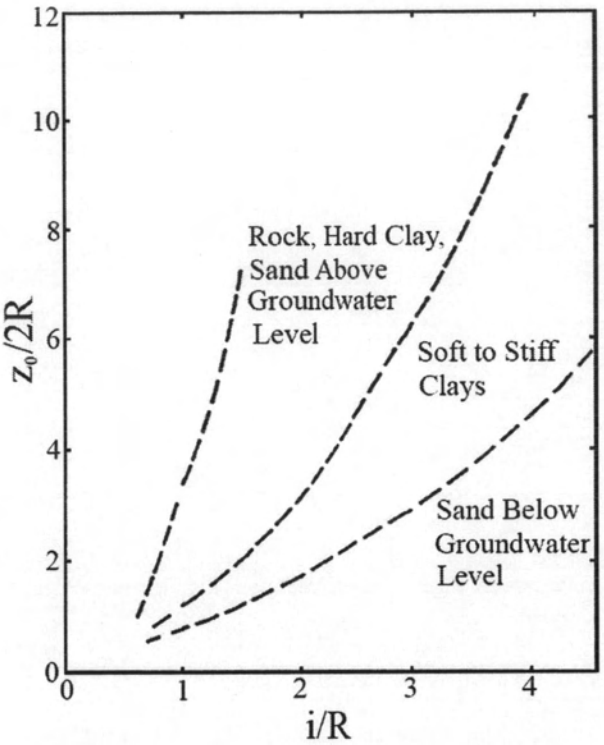

Figure 4.7 Relation between settlement trough width parameter and depth of tunnel for different soil conditions (Peck, 1969)

For practical purposes, O'Reilly and New (1982) bonded the trough width parameter i to the depth of the tunnel axis z_0 by the linear expression:

$$i = K.z_0 \tag{4.2}$$

Where K is an empirical constant of proportionality, depending on the soil type, and z_0 is the depth of tunnel axis below ground surface.

According to settlement data obtained from 19 locations of tunnel in cohesive soils and 16 locations of tunnel in granular soils, which were excavated in the United Kingdom, O'Reilly and New (1982) plotted the trough width parameter, i, versus the tunnel axis below ground level as shown in Figure 4.8. From the linear regression, two empirical relationships were established:

$$i = 0.43.z_0 + 1.1 \qquad \text{for cohesive soils} \tag{4.3}$$

$$i = 0.28.z_0 - 0.1 \qquad \text{for granular soils} \qquad (4.4)$$

The data used to plot in Figure 4.8 cover the tunnel axis ranged from 3.4 m to 34 m and the linear relationship is better define for cohesive soils than for granular soil. As the linear regression lines pass close to the origin, the expression (4.2) is usually preferable for most purposes. In addition, the values of K vary between 0.4 for stiff clay and 0.7 for soft and silty clays. However, for granular materials above the water table K ranges between 0.2 and 0.3. As a general rule, the width of the surface settlement trough is about three times the depth of the tunnel for tunnels in clay strata (Burland et al., 2001).

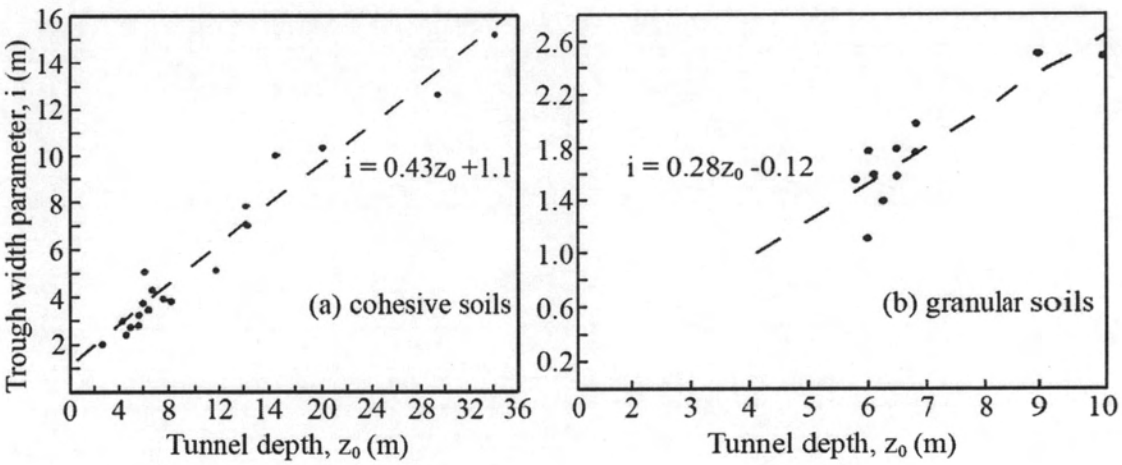

Figure 4.8 Variation of trough width parameter, i, with tunnel depth (O'Reilly and New, 1982)

Pitaksaithong (2001) used the trial error, which is based on the empirical methods of Peck (1969) and O'Reilly and New (1982) to analyze the ground surface settlement caused by a 4.18 m, outer diameter, tunneling in Bangkok subsoils (in a depth of 23.80 m under ground-surface), and he found that i varies from 8 to 12 m, while K varies in the order of 0.34 and 0.50.

The short-term settlements caused by tunnel excavation are typically characterized by the "volume loss" V_L, which is the volume of the surface settlement trough per unit length (V_s) expressed as a percentage of the notional excavated volume of the tunnel. The integration of Equation (4.1) for value of x between $-\infty$ and $+\infty$ is:

$$V_s = \sqrt{2\pi}.i.s_{max} \tag{4.5}$$

Accordingly:

$$V_L = \frac{4.V_s}{\pi.D^2} = \frac{3.192.i.s_{max}}{D^2} \tag{4.6}$$

Where, D is the excavated diameter of the tunnel. Combining Equations (4.1), (4.2), (4.5) and (4.6) gives the surface settlement s at any distance x from the centerline:

$$s = \left(\frac{0.313.V_L D^2}{K.z_o}\right)\exp\left(\frac{-x^2}{2K^2 z_o^2}\right) \tag{4.7}$$

As mentioned previously, the value of s equals the maximum settlement s_{max} at the vertical axis where x equals zero. Above the tunnel axis, therefore, the maximum surface settlement can be written:

$$s_{max} = \frac{0.313.V_L D^2}{K.z_o} \tag{4.8}$$

Besides the surface settlement, Mair et al. (1993) assumed that the shapes of subsurface settlement profiles developed during tunnel construction are characterized by the Gaussian distribution (Equation 4.1), in the same manner as those for surface settlement profiles, and they showed that this assumption is in reasonable agreement with monitored data. However, the substitution of the distance above the tunnel axis (z_0 - z) for z_0 must be done in order to determine the trough width parameter i based on Equation (4.2), where z is a depth from ground surface to the consideration subsurface level (Figure 4.9). Therefore, the Equation (4.2) can be written:

$$i = K.(z_0 - z) \tag{4.9}$$

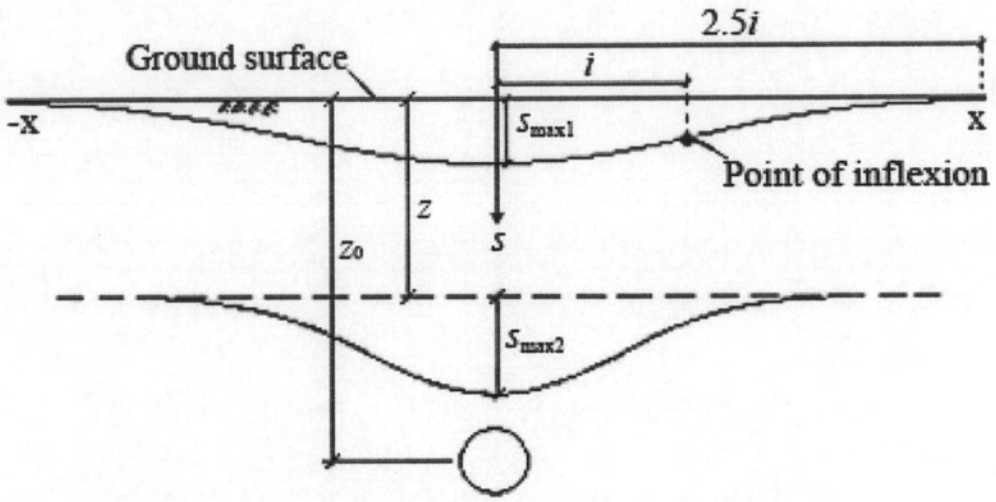

Figure 4.9 Shape of surface and subsurface settlement profiles (Mair et al., 1993)

It is important to note that, even though the value of K for surface settlements is more or less constant for a wide range of tunnel depths in the same ground, its value increases with depth for subsurface settlements and for the tunnels constructed in clays. This argument is shown in Figure 4.10, in which the trough width parameter i obtained from subsurface settlement normalized by z_0 is plotted against depth z, which is also normalized by z_0 (Mair et al., 1993).

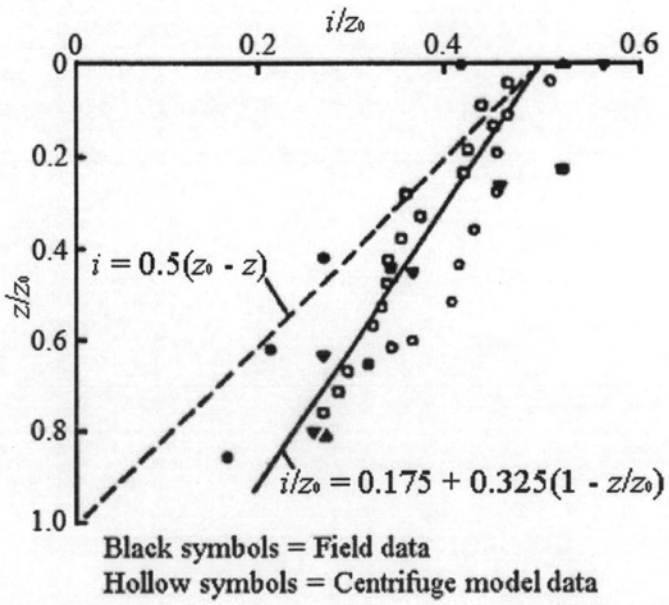

Figure 4.10 Variation of subsurface settlement trough width parameter, i, with depth for tunnel in clays (Mair et al., 1993)

It can be seen that the dash line, which represents Equation (4.9) for various depths of subsurface settlements and for K = 0.5, underestimates the width of subsurface settlement profile. However, the solid line, which is drawn through the data, gives a better estimation of i and is expressed by the following equation:

$$i/z_0 = 0.175 + 0.325(1 - z/z_0) \tag{4.10}$$

Combining Equation (4.9) and (4.10) gives

$$K = \frac{0.175 + 0.325(1 - z/z_0)}{1 - z/z_0} \tag{4.11}$$

The curve expressed by Equation (4.11) is plotted in Figure 4.11, together with the values of K derived from Equation (4.9) using the i values obtained from field measurements and centrifuge model data shown in Figure 4.10. One could see that if K = 0.5 was assumed, it would be underestimated for the large values of z/z_0; consequently, the magnitude of settlement would be overestimated.

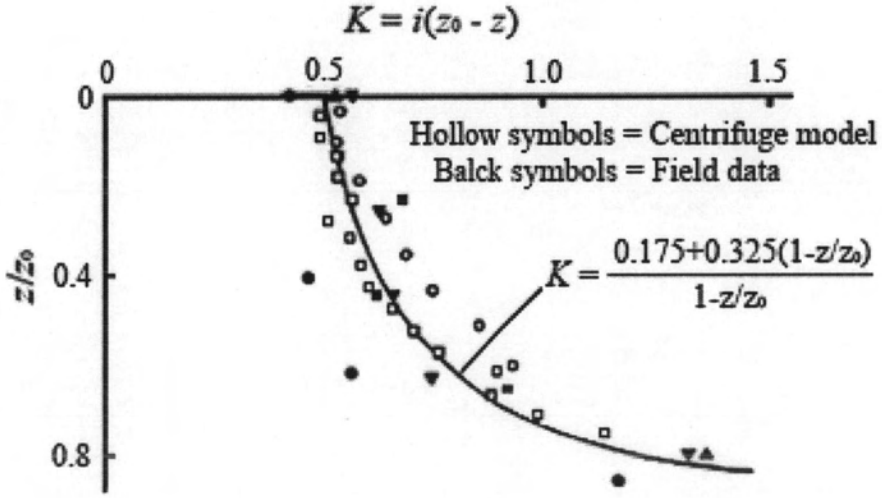

Figure 4.11 Variation of K for subsurface settlement profile with depth above tunnel in clays (Mair et al., 1993)

Combining Equation (4.8) and (4.10), gives the maximum subsurface settlement as

$$\frac{s_{max}}{R} = \frac{1.25V_L}{0.175 + 0.325(1 - z/z_0)} \cdot \frac{R}{z_0} \tag{4.12}$$

where R is the tunnel radius. Figure 4.12 shows the maximum subsurface settlement normalized by the tunnel radius against the tunnel radius normalized by the depth of the considered subsurface level to the tunnel axis, $R/(z_0 - z)$. The field monitored data plotted in the figure were collected from the tunnel construction in London Clay for the radius 2.07 and 3.9 m. However, the tunnel depth was ranged from 20 to 41 m. The line A is plotted based on the Equation 4.8, in which K is taken as 0.5 and z_0 is substituted by $(z_0 - z)$, and the volume of ground loss is assumed to be 1.4%. In addition, the curves B and C are derived from Equation (4.12) for two different ratio of R/z_0 are also plotted in the graph except the solid line, which is drawn based on the plasticity solution given by Mair and Taylor (1993). The Figure clearly shows that the determination of s_{max} for subsurface settlement based on Equation 4.8 for $K = 0.5$ leads to an overestimation.

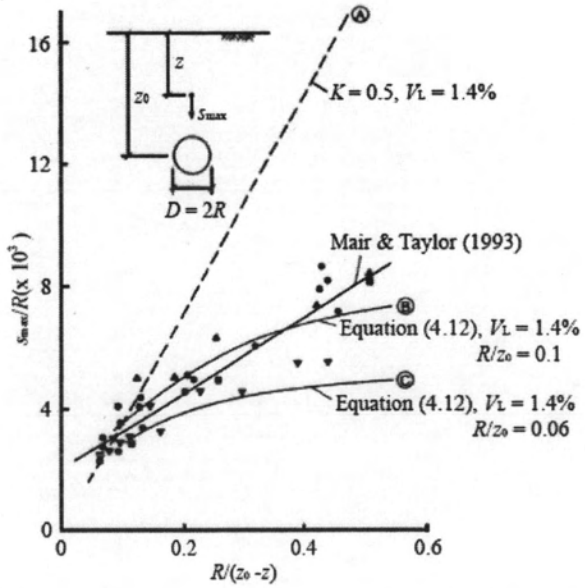

Figure 4.12 Subsurface settlements above the tunnel axis in London Clay (Mair et al., 1993)

In addition to what had been done by Mair et al. (1993), Luangpitakchumpol et al. (2005) reported based on MRTA project and water diversion project (Premprachakorn) in Bangkok subsoils that the maximum subsurface settlement s_{max} did not only vary according to the tunnel depth, but also the tunnel radius itself as shown in Figure 4.13. This correlation; however, is applicable only to shield tunneling in the very stiff silty clay with outer diameter between 4 and 6.5 meters, and the ground loss is limited at the intervals of 1 and 3%.

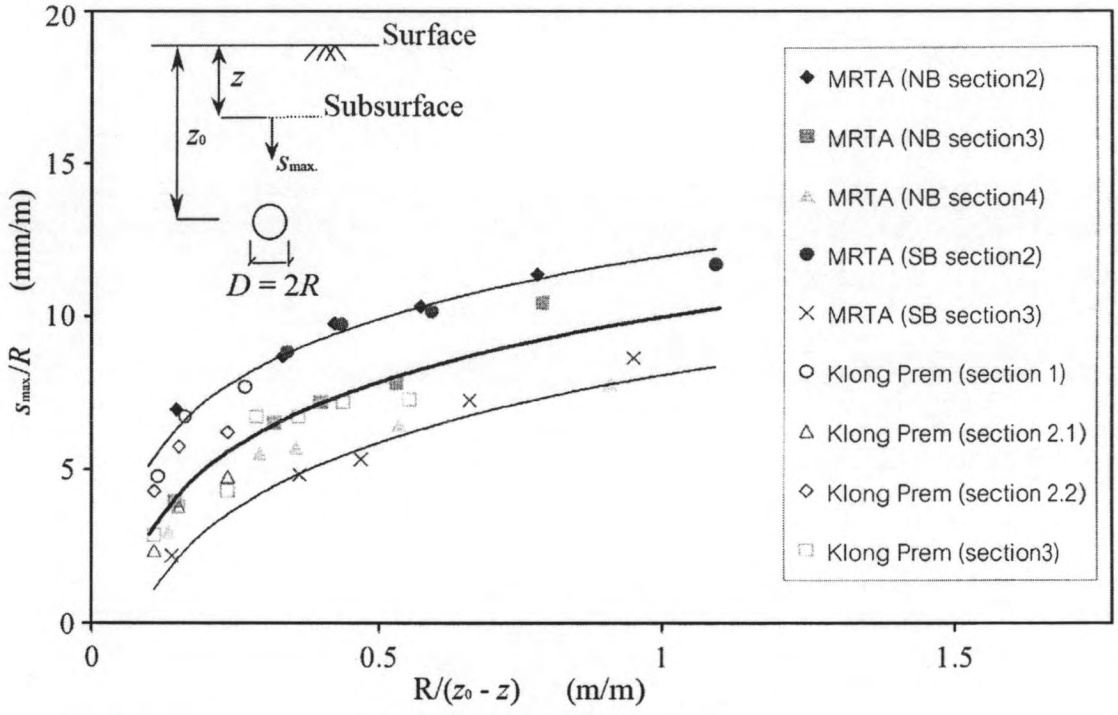

Figure 4.13 Correlation of maximum subsurface settlement (Luangpitakchumpol et al., 2005)

4.2.2 Analytical Methods

Several analytical solutions have been developed in order to predict the movements of ground induced by tunnel excavation. In general, the suggested approaches are usually modified from the basic ideas of the senior or previous researchers, and the important points in those methods vary according to the philosophy and the knowledge of the developers (researchers). In this paragraph, a series of analytical solutions, which have been developed continuously, will be briefly reviewed.

Sagaseta (1987) introduced closed form solutions for obtaining the strain field in an initially isotropic and homogenous incompressible soil (Poisson's ratio equals to 0.5) due to near surface ground loss. The strain controlled and incompressible conditions were mainly considered in the analysis problems. In addition, the virtual image technique was used at the free surface (Figure 4.14). The vertical soil displacement at any levels below ground surface could be defined as

$$s_z = -\frac{V_L}{2\pi}\left(\frac{z-z_0}{r_1^2} - \frac{z+z_0}{r_2^2}\right). \tag{4.13}$$

where V_L is the volume loss, which is expressed as the ratio of the surface settlement trough per meter run of the tunnel area. z_0 is the depth of tunnel axis from ground surface; z is a depth from ground surface to the consideration subsurface level and x is the lateral distance to the tunnel center line. Based on the simple geometry shown in Figure 4.14, the values of r_1^2 and r_2^2 could be known as $[x^2 + (z - z_0)^2]$ and $[x^2 + (z + z_0)^2]$, respectively.

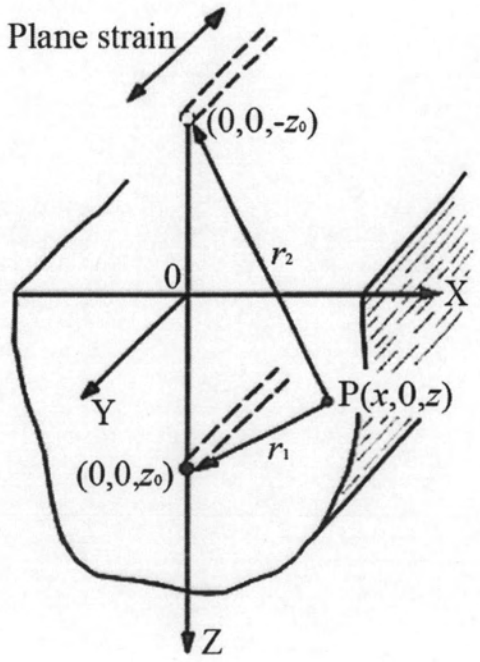

Figure 4.14 Point sink (ground loss) and virtual image technique (Sagaseta, 1987)

At ground surface, the settlement could be expressed as:

$$s = \frac{V_L}{\pi} \cdot \frac{z_0}{x^2 + z_0^2} \tag{4.14}$$

Verruijt and Booker (1996) extended the method suggested by Sagaseta (1987) for the ground loss in an incompressible soil. The solution given by Verruijt-Booker's method is not only applicable for the Poisson's ratio which equals to 0.5 (incompressible soil), but also for the arbitrary values of Poisson's ratio. Furthermore, it includes the effect of ovalization as well. The tunnel in a semi-infinite medium is considered in this approximate analytical solution, and the general ground settlement could be expressed as

$$\begin{aligned} s_z = & -\varepsilon R^2 \left(\frac{z - z_0}{r_1^2} + \frac{z + z_0}{r_2^2} \right) \\ & + \delta R^2 \left[\frac{(z - z_0)\left(kx^2 - (z - z_0)^2\right)}{r_1^4} - \frac{(z + z_0)\left(kx^2 - (z + z_0)^2\right)}{r_2^4} \right] \\ & + \frac{2\varepsilon R^2}{m} \left[\frac{(m+1)(z + z_0)}{r_2^2} - \frac{mz\left(x^2 - (z + z_0)^2\right)}{r_2^4} \right] \\ & - 2\delta R^2 z_0 \left[\frac{x^2 - (z + z_0)^2}{r_2^4} + \frac{m}{m+1} \frac{2z(z + z_0)\left(3x^2 - (z + z_0)^2\right)}{r_2^6} \right] \end{aligned} \tag{4.15}$$

where ε is a parameter indicating the relative uniform radial displacement of the tunnel surface with radius R, and δ is the relative displacement caused by the ovalization of the tunnel. For more comprehensive understanding, the parameters ε and δ are illustrated in Figure 4.15. The distances r_1 and r_2 are shown in Figure 4.14 and can be determined in the same way as those in Equation (4.13); $k = \nu(1 - \nu)$ and the auxiliary elastic constant, m, is related to Poisson's ratio by

$$m = \frac{1}{1 - 2\nu} \tag{4.16}$$

At ground surface, where $z = 0$, the first and second term in the Equation (4.15) are equal to zero. Therefore, the expression for surface settlement could be written as

$$s = 2\varepsilon R^2 \frac{m+1}{m} \frac{z_0}{x^2 + z_0^2} - 2\delta R^2 \frac{z_0(x^2 - z_0^2)}{(x^2 + z_0^2)^2} \tag{4.17}$$

Substituting the Equation (4.16) in (4.17), the surface settlement gives

$$s = 4\varepsilon R^2 (1 - \nu) \frac{z_0}{x^2 + z_0^2} - 2\delta R^2 \frac{z_0(x^2 - z_0^2)}{(x^2 + z_0^2)^2} \tag{4.18}$$

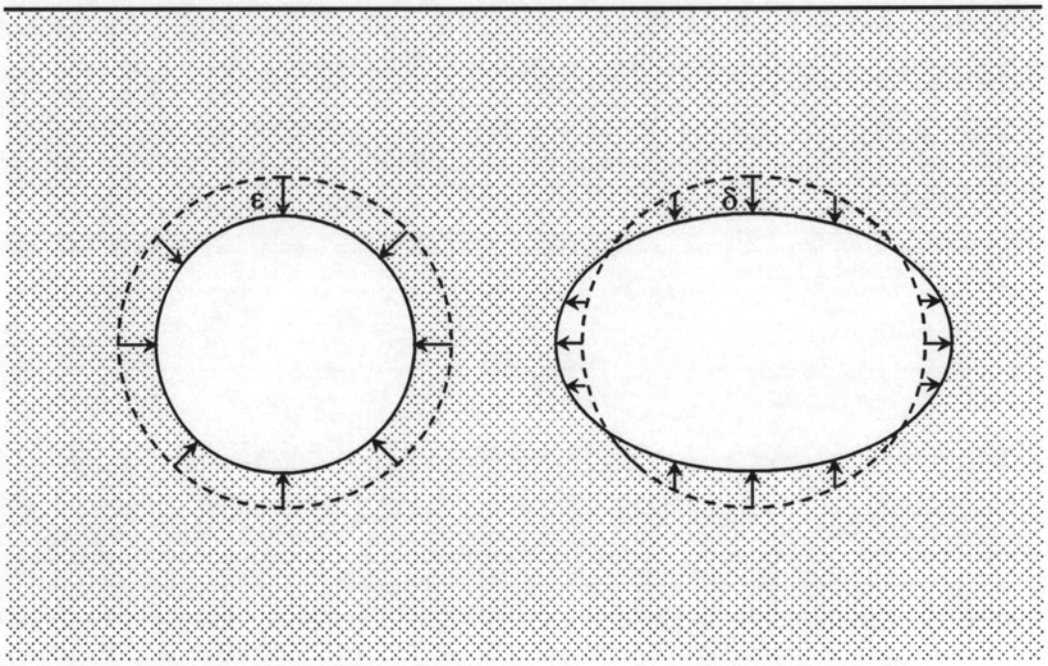

Figure 4.15 Ground loss and ovalization of a tunnel (Verruijt and Booker, 1996)

The total area (A) of settlement trough could be obtained by integrating the above equation (Equation 4.18) from $-\infty$ to $+\infty$. The result is

$$A = 4(1-\nu)\varepsilon\pi R^2 \tag{4.19}$$

So that,

$$\varepsilon = \frac{A}{4(1-\nu)\pi R^2} = \frac{V_L}{4(1-\nu)} \tag{4.20}$$

For the value of Poisson's ratio $\nu = 0.5$, the first term of Equation (4.18) could be converted to Equation (4.14) presented earlier by Sagaseta (1987).

Loganathan and Poulos (1998) redefined the traditional ground loss parameter with respect to gap parameter, G_{AP}, which was presented by Lee et al. (1992), and incorporated to the analytical solution of Verruijt and Booker (1996) to estimate the ground movements around the tunnel in clays. However, only the short-term undrained condition was considered while the ground deformations due to long-term ovalization of the tunnel lining are neglected ($\delta = 0$). Therefore, the short-term surface settlement could be expressed as

$$s = 4R^2(1-\nu)\frac{z_0}{x^2+z_0^2}\frac{4G_{AP}R+G_{AP}^2}{R^2}\exp\left[-\frac{1.38x^2}{(z_0+R)^2}\right] \tag{4.21}$$

where G_{AP} is the gap parameter, and the other parameters are the same as those in the previous equations. The gap parameter could be estimated by

$$G_{AP} = G_p + u^*_{3D} + \omega \tag{4.22}$$

where G_p is the physical gap ($G_p = 2\Delta + \delta$), which represents the geometric clearance between the outer skin of the shield and the lining, Δ is the thickness of tailpiece and δ is the clearance required for erection of lining. The term u^*_{3D} represents the three-dimensional (3D) elastic deformation at the tunnel face and ω takes into account the quality of workmanship. The tunnel heading and 2D plane strain representation of tunnel heading are shown in Figure 4.16. The clearance (δ) for erection of lining indicated in the figure is considered both clearances at crown and invert.

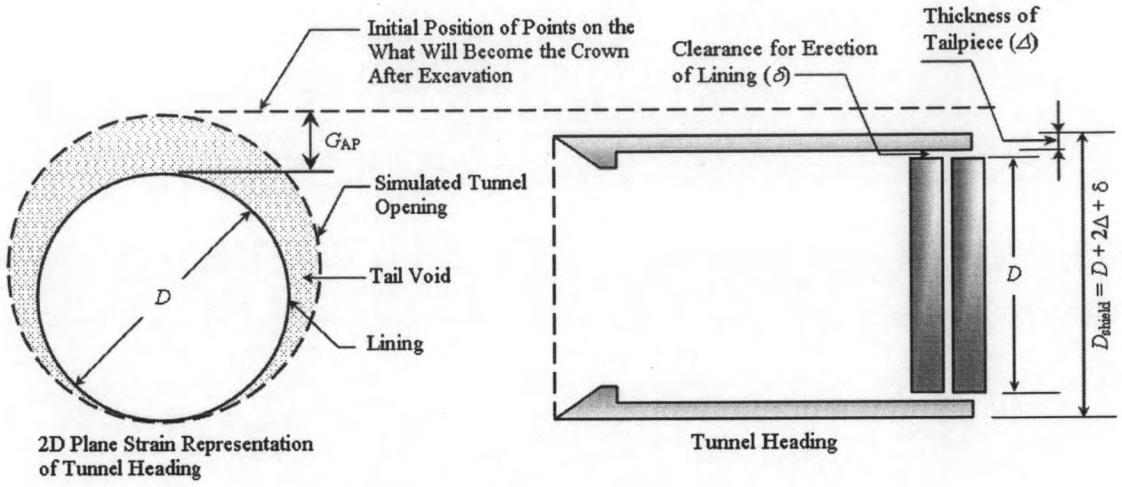

Figure 4.16 Definition G_{AP} (Lee et al., 1992)

Besides the ground surface settlement, Loganathan and Poulos also suggested the subsurface settlement profiles as

$$s_z = R^2\left\{-\frac{z-z_0}{x^2+(z-z_0)^2}+(3-4\nu)\frac{z+z_0}{x^2+(z+z_0)^2} - \frac{2z\left[x^2-(z+z_0)^2\right]}{\left[x^2+(z+z_0)^2\right]^2}\right\}\frac{4G_{AP}R+G_{AP}^2}{4R^2}\exp\left\{-\left[\frac{1.38x^2}{(z_0+R)^2}+\frac{0.69z^2}{z_0^2}\right]\right\} \quad (4.23)$$

It reveals that at ground surface (z = 0), the Equation (4.23) becomes exactly the Equation (4.20).

4.2.3 Laboratory Testing

Within these three decades, some geotechnical researchers have carried out the centrifuge tests in order to study the behaviors of ground responding to the underground opening or to find out the reasons after a collapse of a structure. The centrifugal tests or the imitations of tunnel excavation in laboratory consist of a preparation of a reduced scale model representing the tunnel diameter and its depth below ground surface. For the model tested with an acceleration of α times the Earth gravity (g), the equivalent full scale is α times the dimension in the model. In addition, the geological properties are prepared according to the desired material to be studied;

however, the principle component of tunnel liner is usually made of metal tube such as aluminum. Subsequently, the stress strain in the soil and the behaviors of ground deformations during the simulation could be examined based on the monitoring systems, which were set up in prior to the test. Although some centrifugal tests have been performed on the tunnel constructions, few case studies of these tests are briefly described here.

A series of centrifuge model tests, which could be accelerated to 75g, was performed by Atkison and Potts (1977) to simulate the tunnel excavation in an over consolidated clay and sand. The settlement data obtained from the tests were compared with one and another and with the data monitored above some actual tunnel constructions. Their research led to a suggestion of the following trough width parameter, i, for surface settlement:

- for loose sand

$$i = 0.25(z_0 + R) \tag{4.24}$$

- for dense sand and over consolidated clay

$$i = 0.25(1.5z_0 + 0.5R) \tag{4.25}$$

Loganathan et al. (2000) performed the centrifuge model testing for tunneling in clay in order to monitor the ground deformations, and then they compared the obtained data with the empirical and the analytical methods of estimation. Moreover, the behavior of a single pile and a pile group responding to the tunneling in the model was also observed. The tunnel was modeled by an aluminum tube covered by the rubber membrane and the annulus between the rubber membrane and aluminum tube (inner core of the model tunnel) filled with the silicone oil. By doing this the volume of ground loss was simulated by reducing the volume of silicone oil; thereby, decreasing the diameter of the tunnel. The detail descriptions of the centrifuge model setup were clearly mentioned in that paper. In 2003, in order to study the mechanism of the tunnel face failure of a shallow tunnel in sandy ground (the ratio of the soil cover to the tunnel diameter was fixed to 1) and the effect of the face bolting, vertical pre-reinforcement bolting and forepoling, Kamata and Mashimo (2003) conducted a set of centrifuge model tests. However, only half of cylindrical shell was created for

the model tunnel with 80 mm in diameter and the maximum centrifugal acceleration was limited to 30g. The experimental results were compared with the analytical results by the Distinct Element Method (DEM). One of their findings from the tests is that the forepoling reinforcement is less effective on face stability than the vertical pre-reinforcement bolting. Lee et al. (2006) carried a series of 100g centrifuge model tests to investigate the surface settlement troughs, excess pore water pressure generation, tunnel stability and arching effect built up during tunneling at various depths in clayey soil, which had an untrained shear strength profile of 30-40 kPa. Both single and two parallel tunnels were simulated and the experimental results were also compared with the numerical simulations.

As mentioned earlier in this section (section 4.2), the time consumed for sample preparation and the repetition of the experimentation is lengthy. Furthermore, it is costly and difficult to simulate the real behavior of tunnel excavation as well as to implement the surface and subsurface structures into the reduced scale model since the major structures are made of concrete or brickwork. Therefore, the numerical simulation is more advantageous regarding to these problems. However, these physical model tests still play an important role in providing the data for verifying and comparing the behaviors of ground movements with the existing methods, especially with the numerical analyses.

4.2.4 Numerical Analysis Methods

The prediction of ground movements in response to tunneling based on the empirical and analytical methods as well as the laboratory tests have been reviewed in the previous sections. However, those approaches were restricted to only tunneling below green field site, which are not always realistic for urban areas. The problems encountered for tunnel excavation in such locations could be cited as existing surface structures (buildings) and underground structures, which are tunnels, underground stations and pile foundations. In these situations, numerical or finite element method provides a huge advantage to input all the elements in question into one model and the ground deformations as well as the interaction between soil-structures and structures-structures could be studied. This section introduces a brief overview of the application of finite element method (FEM) to predict the ground movements caused by tunneling.

The finite element method has been used in many field of engineering practice for around forty year; however, it has begun to be widely used for analyzing geotechnical problems recently. This is probably because there are many complex issues which are specific to geotechnical engineering and which have been solved recently (Potts and Zdravković, 1999). This method consists of discretisation of a continuum into finite elements and each element has a number of nodes, which serve as connectors that fasten elements together. It is noticeable that all elements sharing a node have the same displacement components on that node.

The primary characteristics of a finite element are embodied in the element stiffness matrix. The stiffness matrix contains the geometric and material behavior information that indicates the resistance of the element to deformation when is subject to loading or external influences (Hutton, 2004).

The tunnel excavation is a 3D issue, but the 3D-FE analysis usually leads to an excessive time consuming and high capacity of storage. In practice, therefore, the 2D computation is much more preferable. Several methods have been suggested to model the tunnel excavation, and the most well known methods are briefly described in the following paragraph:

The gap method: this method was originally mentioned by Rowe et al. (1983). The expected volume loss is modeled by establishing a pre-described void into the finite element mesh, around the final tunnel perimeter. However, the invert of final tunnel lining must be in touch with the underlying soil as shown in Figure 4.16 of section 4.2.2. The tunnel excavation is simulated by removing the soil clusters inside the tunnel and around its periphery, and then the soil displacement is allowed until the gap is closed. As mentioned in section 4.2.2, the predefined gap parameter (G_{AP}) depends on the tunneling machine and lining parameters, soil type and quality of workman ship. The lower limit of gap parameter could be estimated as the difference between the outer diameter of the tunneling machine and the outer diameter of the lining.

The convergence-confinement method: this method was introduced by Panet and Guenot (1982); it is also called λ method. The parameter λ describes the proportion before the tunnel lining is constructed. At the initial condition, the pressure exerted on the tunnel boundary by the soil to be excavated is equal to σ_0 (initial soil tress), and λ is equal to 0. λ is then gradually increased to 1 to simulate the tunneling

process. During the tunnel excavation, the pressure at the lining boundary is reduced with a numbers of increment to $(1-\lambda)\sigma_0$. After lining erection, the remainder of stress reduction is still applied to create the lining stress. The stress reduction with the tunnel lining in place is, therefore, equals $(1-(1-\lambda))\sigma_0$ or $\lambda\sigma_0$, where λ continues to increase from the end of excavation step. Finally, the initial stress is then introduced into the tunnel lining. In this method, the ground loss is a predicted value. To achieve the desired ground loss, the installation of lining must be done at an appropriate calculation increment by taking into account the stiffness of the lining as well. It is noticeable that the desired ground loss given by the ground displacement normal to the tunnel perimeter should be equal to ground loss in an undrained greenfield excavation.

The progressive softening method: this method was developed for modeling of tunnel excavation using the New Austrian Tunneling Method (NATM) by Swoboda (1979). Unlike the convergence-confinement method, the tunnel excavation based on this method was simulated by reducing the stiffness soil clusters inside the future tunnel boundary.

The volume loss control method: in this method, the expected ground loss that will result on completion of excavation is prescribed prior to lining construction. This method is used to predictive analyses of tunnel excavation for which the ground loss can be determined for a given tunneling method. Moreover, it is found to be very useful for back analysis of tunnel excavation when the ground loss have been monitored (Potts and Zdravković, 2001).

The tunnel lining contraction method: If a circular tunnel is to be analyzed, a contraction of the tunnel lining (shrinkage) can be prescribed to simulate the ground loss in response to the boring process. The contraction is expressed in percentage as a ratio of the area reduction and the original outer tunnel cross section area (Brinkgreve, 2002). The application of this method is similar to the volume loss control method; however, the contraction is specified to the lining after it has been installed (activated).

Among the above mentioned methods, the simulation of tunnel excavation as well as the prediction of ground movements based on the lining contraction method is found to be much more convenient. A detail section about this last method and the overview of finite element program used for this research is described in Chapter VI.

4.3 Appropriate Methods for Analyses of the Research Project

For the fact that the analytical solutions employ more parameters, it is not always easy to estimate during the design phase. Moreover, for those analyses based on gap parameter (G_{AP}), Rowe et al. (1983) mentioned that the G_{AP} is the most critical and difficult parameter to determine. Thus, these approaches will not be considered in the analysis phases of this research. Regarding the laboratory or centrifuge test, besides time consuming, high cost, the difficulty to implement the surface and subsurface structures which are made of concrete or masonry into the model, the facility is not yet available in our laboratory. Therefore, the potential for analyses the ground surface settlements in this research will refer to the empirical approach (Peck, 1969), which has been extensively used for this purpose. Furthermore Rowe and Kack (1983) acknowledged that the empirical relationships may yield quite adequate and economical design when they are applied with appropriate judgment based on similar past experiences. At the same time, the FE analysis method will cover both ground surface and subsurface settlements as well as the structural settlements. In addition, the internal forces of the tunnel liner could be achieved as well.